J. Fluid Mech. (2003), *vol.* 495, *pp.* 193–208.
DOI: 10.1017/S0022112003006141 Printed in the United Kingdom

Rapid shear flows of dry granular masses down curved and twisted channels

By SHIVA P. PUDASAINI AND KOLUMBAN HUTTER

Department of Applied Mechanics, Institute for Mechanics-AG III,
Darmstadt University of Technology, Hochschulstrasse 1, D-64289, Germany

(Received 31 May 2002 and in revised form 8 July 2003)

This paper presents a two-dimensional depth-integrated theory for the gravity-driven free-surface flow of a granular avalanche over an arbitrarily but gently curved and twisted topography which is an important extension of the original Savage & Hutter theory. In contrast to previous extensions the present coordinate system is based on a reference curve with curvature and torsion. Its derivation was necessary because real avalanches are often guided by rather curved and twisted valleys or more general slopes. The aim is to gain fundamental insight into the effects of non-uniform curvature and torsion, using an orthogonal coordinate system that rotates with torsion, and find an analytic description of flow avalanches. We present a set of model equations which comprises nonlinear hyperbolic partial differential equations for the space and time evolution of the granular pile height and the depth-averaged streamwise velocity distribution of a finite mass of granulates. The emerging theory is believed to be capable of predicting the flow of dense granular materials over moderately curved and twisted channels of general type.

1. General introduction

Avalanches can physically be characterized as multiphase gravity flows, which consist of randomly dispersed interacting phases, whose properties change with respect to both time and space (Lang & Dent 1980, 1982). Thus, an avalanche can be described as a transient, three-dimensional gravity-driven free-surface motion of a mass system made up of an assemblage of granular fragments initiated by an instability of a granular layer and flowing down to the run-out zone on an arbitrarily steep topography with any surface resistance. In this sense, an exact analysis of an avalanche is perhaps an unattainable goal although the last few years have witnessed increased efforts devoted to the physical understanding of avalanche formation and motion in complex topography.

The study of granular avalanches is very important both in natural environments and in industrial flows. Rockfalls, landslides, debris and snow-slab avalanches are some examples of granular avalanches in geophysical contexts. Similarly, flows in silos, hoppers, rotating drums and slag heaps are examples in industrial applications. Although there may be a great difference in length scale between the geophysical and industrial avalanches the dominant physical mechanisms that drive the flow are similar. Because of their practical importance, granular flows and avalanches have been studied by many researchers from different disciplines, who each present models (see, e.g., Jenkins & Savage 1983; Jenkins & Richman 1985; Hutter & Rajagopal 1994; Herrmann & Luding 1998; Pudasaini & Mohring 2002).

1.1. *A continuum mechanical theory*

It is probably fair to state that Savage & Hutter (1989, 1991), developed the first continuum mechanical theory capable of describing the evolving geometry of a finite mass of a granular material and the associated velocity distribution as an avalanche slides down inclined surfaces. Several simplifying, but nevertheless realistic, assumptions were made, as follows. The moving and deforming granular mass is supposed to be cohesionless, volume preserving and obeys a Mohr–Coulomb yield criterion both inside the mass and at the sliding basal surface. The geometry of the avalanching mass is shallow in the sense that the typical avalanche thickness is small in comparison to the extent parallel to the sliding surface. The motion consists of shearing within the deforming mass and sliding along the basal surface. However, on the basis of observations the shearing deformation commonly takes place within a very small basal boundary layer, so that it is justified to collapse this layer to zero thickness and to combine the sliding and shearing velocity into a single sliding law with somewhat larger modelled sliding velocity. The theory has been generalized to higher dimensions and was tested against laboratory experiments. Good agreements were obtained between the theoretical predictions and experiments, proving it to be adequate as one of the leading mathematical models for an avalanche (Hutter & Koch 1991; Greve & Hutter 1993; Hutter *et al.* 1993; Greve, Koch & Hutter 1994; Koch, Greve & Hutter 1994; Gray, Wieland & Hutter 1999; Wieland, Gray & Hutter 1999; Gray 2001; Pudasaini, Eckart & Hutter 2003*a*; Pudasaini, Hutter & Eckart 2003*b*).

1.2. *Present model*

In the present contribution we have extended the Savage–Hutter (SH) theory to rapid shear flows of granular avalanches in a non-uniformly curved and twisted channel. An orthogonal coordinate system along a 'generic master curve' can be introduced and the (SH) equations can be explicitly derived in this frame of reference. We are, thus, able to study the simultaneous effects of curvature and torsion on the flow avalanche in channels which could not be investigated before. This makes the present model applicable to realistic avalanche motions down arbitrary guiding topographies such as valleys and channelised corries. In fact, Geographic Information Systems (GIS) applied to mountainous avalanche-prone regions can be applied to this model. This paper provides the theoretical foundation for an application close to realistic situations and tuned to practical use.

2. Field equations

The avalanche is assumed to be an incompressible material with constant bulk density ϱ_0. Then the mass and momentum conservation laws reduce to

$$\nabla \cdot \boldsymbol{u} = 0, \qquad \varrho_0 \left\{ \frac{\partial \boldsymbol{u}}{\partial t} + \nabla \cdot (\boldsymbol{u} \otimes \boldsymbol{u}) \right\} = -\nabla \cdot \boldsymbol{p} + \varrho_0 \boldsymbol{g}, \tag{2.1a, b}$$

where $\boldsymbol{u}$ is the velocity, $\otimes$ the tensor product, $\boldsymbol{p}$ the pressure tensor and $\boldsymbol{g}$ the gravitational acceleration. The granular avalanche is assumed to satisfy a Mohr–Coulomb yield criterion in which the internal shear stress $\boldsymbol{S}$ and the normal pressure N are related by

$$|\boldsymbol{S}| = N \tan \phi, \tag{2.2}$$

where ϕ is the internal angle of friction. The conservation laws (2.1*a*) and (2.1*b*) are

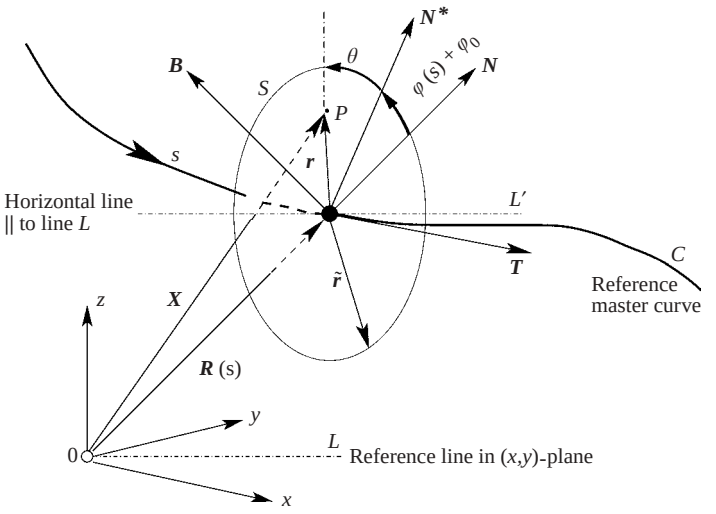

FIGURE 1. $\boldsymbol{R}(s)$ describes the reference curve C embedded in $\mathbb{R}^3$. s is the arclength, $\{\boldsymbol{T}, \boldsymbol{N}, \boldsymbol{B}\}$ is the moving orthonormal unit triad following the curve. (r, θ) are polar coordinates spanning the plane of circle S with radius $\tilde{r}$ normal to the axis of the master curve C. The origin of the azimuthal angle, θ, in this plane is arbitrary, but measured from the unit vector $\boldsymbol{N}^*$ which is rotated from $\boldsymbol{N}$ by a phase $(\varphi(s)+\varphi_0)$ for $s \in [s_0, \infty)$, $s_0 \in [0, \infty)$ and $\theta \in (0, 2\pi]$. Also φ_0 is an arbitrary constant and P is any point in space.

complemented by kinematic boundary conditions

$$\frac{\partial F^s}{\partial t} + \boldsymbol{u}^s \cdot \nabla F^s = 0, \qquad \frac{\partial F^b}{\partial t} + \boldsymbol{u}^b \cdot \nabla F^b = 0, \tag{2.3a, b}$$

where the superscripts s and b indicate that a variable is evaluated at the surface, $F^s(\boldsymbol{x}, t) = 0$, and the base, $F^b(\boldsymbol{x}, t) = 0$, respectively. The free surface of the avalanche is traction free while the base satisfies a Coulomb dry-friction sliding law. That is,

$$\boldsymbol{p}^s \boldsymbol{n}^s = \boldsymbol{0}, \qquad \boldsymbol{p}^b \boldsymbol{n}^b - \boldsymbol{n}^b (\boldsymbol{n}^b \cdot \boldsymbol{p}^b \boldsymbol{n}^b) = (\boldsymbol{u}^b / |\boldsymbol{u}^b|)(\boldsymbol{n}^b \cdot \boldsymbol{p}^b \boldsymbol{n}^b) \tan \delta, \tag{2.4a, b}$$

where $\boldsymbol{n}^s$ and $\boldsymbol{n}^b$ are outward normals, and δ is the basal angle of friction.

3. Coordinate system

Consider an avalanche-prone landscape and a subregion of it where the topography allows the identification of an avalanche track. A single curve, following the landscape topography (e.g. the talweg of the valley) is selected as a master (reference) curve C from which the track topography will be modelled. Let this three-dimensional curve be smooth and be given by $\boldsymbol{R}(x, y, z)$, where x, y and z are the Cartesian coordinates. A curvilinear coordinate system is constructed (see, e.g., Germano 1982, 1989; Zabielski & Mestel 1998a, b) by considering this spatial curve to be described by the position vector $\boldsymbol{R}(s)$, where s is the arclength. At any point of the curve we have the orthonormal triad $\{\boldsymbol{T}, \boldsymbol{N}, \boldsymbol{B}\}$ which, respectively, comprises the tangent, normal and binormal unit vectors, also expressible as functions of s. The vector pair $\{\boldsymbol{N}, \boldsymbol{B}\}$ spans a plane perpendicular to C. Any vector $\boldsymbol{X}$ in the three-dimensional space can be expressed as

$$\boldsymbol{X} := \boldsymbol{X}(s, r, \theta) = \boldsymbol{R}(s) + r \cos(\theta + \varphi(s) + \varphi_0)\boldsymbol{N}(s) + r \sin(\theta + \varphi(s) + \varphi_0)\boldsymbol{B}(s). \tag{3.1}$$

Here, (r, θ) are polar coordinates spanning the plane normal to the axis of C in figure 1. The origin of the azimuthal angle, θ, in this plane is arbitrary, but measured from

the unit vector $\boldsymbol{N}^*$ which is rotated from $\boldsymbol{N}$ by a phase $(\varphi(s)+\varphi_0)$. Also, φ_0 is an arbitrary constant and

$$\varphi(s) = -\int_{s_0}^{s} \tau(s')\,\mathrm{d}s'. \tag{3.2}$$

Hence the torsion, $\tau(s)$, enters into the equations through the auxiliary function $\varphi=\varphi(s)$. From differential geometry we recall the following results:

$$\boldsymbol{T}(s) = \frac{\mathrm{d}\boldsymbol{R}(s)}{\mathrm{d}s}, \quad \boldsymbol{N}(s) = \frac{1}{\kappa}\frac{\mathrm{d}\boldsymbol{T}(s)}{\mathrm{d}s}, \quad \boldsymbol{B}(s) = \boldsymbol{T}(s)\times\boldsymbol{N}(s), \tag{3.3}$$

where κ is the curvature of the curve C. Curvature and torsion can be computed from $\boldsymbol{R}=\boldsymbol{R}(x,y,z)$ and are expressible as functions of the arclength s: $\kappa=\kappa(s)$ and $\tau=\tau(s)$. The Serret–Frénet formula provides a connection between the curvature and torsion and the changes of $\boldsymbol{T}$, $\boldsymbol{N}$, $\boldsymbol{B}$ along s as follows:

$$\frac{\mathrm{d}\boldsymbol{T}}{\mathrm{d}s} = \kappa\boldsymbol{N}, \quad \frac{\mathrm{d}\boldsymbol{N}}{\mathrm{d}s} = \tau\boldsymbol{B}-\kappa\boldsymbol{T}, \quad \frac{\mathrm{d}\boldsymbol{B}}{\mathrm{d}s} = -\tau\boldsymbol{N}. \tag{3.4}$$

One can easily show that the metric for the chosen coordinate system is given by

$$\mathrm{d}\boldsymbol{X}\cdot\mathrm{d}\boldsymbol{X} = [1-\kappa(s)r\cos(\theta+\varphi(s)+\varphi_0)]^2(\mathrm{d}s)^2+(\mathrm{d}r)^2+(r\,\mathrm{d}\theta)^2. \tag{3.5}$$

This corroborates the orthogonality of (3.1) and (3.3). This system of coordinates is well known in studies on hydromagnetic equilibria, plasma confinement in closed magnetic systems, the treatment of the Navier–Stokes equations for an incompressible viscous fluid and extension of the Dean equations to helical pipe flow (Dean 1927, 1928; Mercier 1963; Solove'v & Shafranov 1970; Germano 1982, 1989; Gammack & Hydon 2001).

For ease of notation the identities $(x^1,x^2,x^3)=(s,\theta,r)$ will be made. The tangent vectors to the coordinate lines, $\boldsymbol{g}_i=\partial\boldsymbol{X}/\partial x^i$, are given by

$$\boldsymbol{g}_1 = (1-\kappa r\eta)\boldsymbol{T}(s), \quad \boldsymbol{g}_2 = -r\zeta\boldsymbol{N}(s)+r\eta\boldsymbol{B}(s), \quad \boldsymbol{g}_3 = \eta\boldsymbol{N}(s)+\zeta\boldsymbol{B}(s), \tag{3.6}$$

$$\eta = \cos(\theta+\varphi(s)+\varphi_0), \quad \zeta = \sin(\theta+\varphi(s)+\varphi_0). \tag{3.7}$$

The covariant metric coefficients, defined as $g_{ij}=\boldsymbol{g}_i\cdot\boldsymbol{g}_j$ and the associated contravariant metric $(g^{ij})=(g_{ij})^{-1}$ are found to be

$$(g_{ij}) = \begin{pmatrix}(1-\kappa r\eta)^2 & 0 & 0\\ 0 & r^2 & 0\\ 0 & 0 & 1\end{pmatrix}, \quad (g^{ij}) = \begin{pmatrix}1/(1-\kappa r\eta)^2 & 0 & 0\\ 0 & 1/r^2 & 0\\ 0 & 0 & 1\end{pmatrix}. \tag{3.8}$$

The covariant unit vectors are defined as $\boldsymbol{g}_i^*=\boldsymbol{g}_i/\sqrt{g_{(ii)}}$. The Christoffel symbols of the second kind are needed in order to transfer the equations of motion to the curvilinear coordinates. They are defined as (see, e.g., Klingbeil 1966)

$$\Gamma^k_{lm} = \tfrac{1}{2}g^{(kk)}(g_{mk,l}+g_{kl,m}-g_{lm,k}), \tag{3.9}$$

in which the Einstein summation convention is dropped for the bracketed indices. For the curvilinear coordinates (3.8) the components of the Christoffel symbol are

$$\left.\begin{aligned}\boldsymbol{\Gamma}^1 &= -\psi\begin{pmatrix}\Lambda r & -\kappa r\zeta & \kappa\eta\\ -\kappa r\zeta & 0 & 0\\ \kappa\eta & 0 & 0\end{pmatrix}, \quad \boldsymbol{\Gamma}^2 = \frac{1}{r}\begin{pmatrix}-\kappa\zeta/\psi & 0 & 0\\ 0 & 0 & 1\\ 0 & 1 & 0\end{pmatrix},\\ \boldsymbol{\Gamma}^3 &= \begin{pmatrix}\kappa\eta/\psi & 0 & 0\\ 0 & -r & 0\\ 0 & 0 & 0\end{pmatrix},\end{aligned}\right\} \tag{3.10}$$

where

$$\Lambda = \kappa'\eta + \kappa\tau\zeta, \quad \psi = 1/(1-\kappa r\eta), \quad \kappa' = \partial\kappa/\partial s. \tag{3.11}$$

Further, the vector differential operator ∇ is defined as $\nabla = \boldsymbol{g}^k \partial/\partial x^k$, and the gradient of a given scalar field F can be expressed as

$$\nabla F = \psi \frac{\partial F}{\partial s}\boldsymbol{g}_1^* + \frac{1}{r}\frac{\partial F}{\partial \theta}\boldsymbol{g}_2^* + \frac{\partial F}{\partial r}\boldsymbol{g}_3^*. \tag{3.12}$$

The divergence of a vector field $\boldsymbol{u} = u^i \boldsymbol{g}_i$ and a symmetric second-order pressure tensor $\boldsymbol{p} = p^{ij}\boldsymbol{g}_i \otimes \boldsymbol{g}_j$, respectively, are expressed as

$$\nabla \cdot \boldsymbol{u} = \left(\boldsymbol{g}^k \frac{\partial}{\partial x^k}\right) \cdot (u_i \boldsymbol{g}_i) = u^i_{,i} + u^i \Gamma^k_{ik}, \quad \Gamma^k_{ik} = \boldsymbol{g}^k \cdot \boldsymbol{g}_{i,k}, \tag{3.13}$$

$$\nabla \cdot \boldsymbol{p} = \left(\boldsymbol{g}^k \frac{\partial}{\partial x^k}\right) \cdot (p^{ij}\boldsymbol{g}_i \otimes \boldsymbol{g}_j) = \left\{p^{ki}_{,k} + p^{ji}\Gamma^k_{jk} + p^{kj}\Gamma^i_{jk}\right\}\sqrt{g_{(ii)}}\boldsymbol{g}_i^*. \tag{3.14}$$

For notational brevity and to make the present theory compatible with previous theories we define the following new variables, and from now on all derivations use those:

$$(x, y, z) := (s, r\theta, r). \tag{3.15}$$

First we take the differentials with respect to these variables and then we again shift the z-coordinate by an amount z_T, i.e. we replace z by $z + z_T$, where z_T is the distance between the master curve and the talweg. Therefore, (x, y, z) are, from now on, not Cartesian components, but rather the coordinates of the curved and twisted channel, and the origin of this new coordinate system lies in the talweg. Furthermore, the manifold $z = \text{const.}$ forms a curved reference surface and the new z is the coordinate in the direction normal to it. We refer to the x-, y- and z-coordinates as downslope, cross-slope and normal directions, respectively. In the following computations we write

$$\mathscr{Z} = z + z_T. \tag{3.16}$$

With physical components $u^{i*} = u^i\sqrt{g_{(ii)}}$ and $p^{ij*} = p^{ij}(\sqrt{g_{(ii)}}\sqrt{g_{(jj)}})$, (3.13) and (3.14) in curvilinear coordinates, respectively, are

$$\nabla \cdot \boldsymbol{u} = \frac{\partial}{\partial x}(\psi u^{1*}) + \frac{\partial u^{2*}}{\partial y} + \frac{\partial u^{3*}}{\partial z} - \psi^2 \Lambda \mathscr{Z} u^{1*} + \psi\kappa\zeta u^{2*} - \left(\psi\kappa\eta - \frac{1}{\mathscr{Z}}\right)u^{3*}, \tag{3.17}$$

$$\begin{aligned}\nabla \cdot \boldsymbol{p} = {} & \left[\frac{\partial}{\partial x}(\psi p^{11*}) + \frac{\partial p^{12*}}{\partial y} + \frac{\partial p^{13*}}{\partial z} - \psi^2\Lambda\mathscr{Z}p^{11*} + 2\psi\kappa\zeta p^{12*} - 2\psi\kappa\eta p^{13*} + \frac{1}{\mathscr{Z}}p^{13*}\right]\boldsymbol{g}_1^* \\ & + \left[\frac{\partial}{\partial x}(\psi p^{12*}) + \frac{\partial p^{22*}}{\partial y} + \frac{\partial p^{23*}}{\partial z} - \psi\kappa\zeta p^{11*} - \psi^2\Lambda\mathscr{Z}p^{12*} + \psi\kappa\zeta p^{22*}\right. \\ & \left. - \left(\psi\kappa\eta - \frac{2}{\mathscr{Z}}\right)p^{23*}\right]\boldsymbol{g}_2^* + \left[\frac{\partial}{\partial x}(\psi p^{13*}) + \frac{\partial p^{23*}}{\partial y} + \frac{\partial p^{33*}}{\partial z} + \psi\kappa\eta p^{11*}\right. \\ & \left. - \frac{1}{\mathscr{Z}}p^{22*} - \psi^2\Lambda\mathscr{Z}p^{13*} + \psi\kappa\zeta p^{23*} - \left(\psi\kappa\eta - \frac{1}{\mathscr{Z}}\right)p^{33*}\right]\boldsymbol{g}_3^*.\end{aligned} \tag{3.18}$$

4. Non-dimensional equations

The physical components of $\boldsymbol{u}$ are defined as u, v and w. Similarly, p_{xx}, p_{yy}, p_{zz}, p_{xy}, p_{xz} and p_{yz} are, now and henceforth, physical components of $\boldsymbol{p}$. Also, from now on,

we simply write $\boldsymbol{g}_i$ for $\boldsymbol{g}_i^*$, so that $\boldsymbol{u} = u\boldsymbol{g}_x + v\boldsymbol{g}_y + w\boldsymbol{g}_z$ defines physical components. The physical variables are non-dimensionalized by using the scalings

$$\left.\begin{aligned}
&(x, y, z, F^s, F^b, t) = \left(L\hat{x}, L\hat{y}, H\hat{z}, H\hat{F}^s, H\hat{F}^b, (L/g)^{1/2}\hat{t}\right),\\
&(u, v, w) = (gL)^{1/2}(\hat{u}, \hat{v}, \varepsilon\hat{w}),\\
&(p_{xx}, p_{yy}, p_{zz}) = \varrho_0 g H(\hat{p}_{xx}, \hat{p}_{yy}, \hat{p}_{zz}),\\
&(p_{xy}, p_{xz}, p_{yz}) = \varrho_0 g H\mu(\hat{p}_{xy}, \hat{p}_{xz}, \hat{p}_{yz}),\\
&(g_x, g_y, g_z) = g(\hat{g}_x, \hat{g}_y, \hat{g}_z),\\
&(\kappa, \tau) = (\hat{\kappa}/\mathscr{R}, \hat{\tau}/\mathscr{R}_\tau),
\end{aligned}\right\} \tag{4.1}$$

where the hats represent non-dimensional variables. The scalings (4.1) assume that the avalanche has a typical length L tangential to the reference surface and a typical thickness H normal to it. Furthermore, $\mathscr{R}$ and $\mathscr{R}_\tau$ are, respectively, a typical radius of curvature and torsion of the reference geometry. Assuming a granular static balance, the typical normal pressures at the base of the avalanche are of the order $\varrho_0 g H$,† and the Coulomb dry-friction law suggests that the basal shear stresses are of the order $\varrho_0 g H \tan\delta_0$, where δ_0 is a typical basal angle of friction. Also notice that g_x, g_y and g_z in these equations are dimensional physical components of the gravitational acceleration along the x-, y- and z-coordinates, respectively. Finally, the curvature κ and torsion τ are assumed to be of order $1/\mathscr{R}$ and $1/\mathscr{R}_\tau$, respectively. These scalings introduce the following non-dimensional parameters:

$$\varepsilon = H/L, \quad \lambda = L/\mathscr{R}, \quad \lambda_\tau = L/\mathscr{R}_\tau, \quad \mu = \tan\delta_0, \tag{4.2}$$

where ε is the aspect ratio of the avalanche, λ and λ_τ are the measures of the curvature and torsion of the reference geometry with respect to the length of the avalanche and μ is the coefficient of friction of the granular material associated with the base.

4.1. *Balance equations*

Applying the scalings (4.1) and (4.2), it follows that the non-dimensional curvilinear form of the mass balance equation (3.17) is

$$\frac{\partial}{\partial x}(\psi u) + \frac{\partial v}{\partial y} + \frac{\partial w}{\partial z} - \varepsilon\lambda\psi^2\Lambda\mathscr{Z}u + \lambda\psi\kappa\zeta v - (\varepsilon\lambda\psi\kappa\eta - 1/\mathscr{Z})w = 0, \tag{4.3}$$

where the hats are now and henceforth dropped and

$$\psi = 1/(1 - \varepsilon\lambda\kappa\eta\mathscr{Z}), \quad \theta = y/(\varepsilon z_T), \quad \Lambda = (\kappa'\eta + \lambda_\tau\kappa\tau\zeta). \tag{4.4a–c}$$

The momentum balance equation (2.1b) can be written in curvilinear coordinates by using relation (3.18) to transform the tensor $\boldsymbol{u}\otimes\boldsymbol{u}$ and the divergence of the pressure $\boldsymbol{p}$. Let g_x, g_y and g_z be the non-dimensional physical components of the gravitational acceleration along the x-, y- and z-coordinates, respectively. They can be determined as known functions of curvature and torsion referred to the moving triad of the given master curve (or the talweg). Their derivation is given in the Appendix. It follows that the non-dimensional curvilinear momentum components

† This scaling for the normal pressure tacitly assumes a 'hydrostatic nature' of the pressure in a granular heap. This is in fact untypical for granular systems for which the pressure is not the overburden weight but saturates after a certain depth. In hoppers etc. the overburden pressure mg over the whole base (A, say) must equal $\int p\,\mathrm{d}A = mg = \int \varrho_0 g H\,\mathrm{d}A$. So this scaling will always be true, the only exception being if the avalanche is spreading out very rapidly.

in the downslope, cross-slope and normal directions to the reference surface are, respectively,

$$\frac{\partial u}{\partial t}+\frac{\partial}{\partial x}(\psi u^2)+\frac{\partial}{\partial y}(uv)+\frac{\partial}{\partial z}(uw)-\varepsilon\lambda\psi^2\Lambda\mathscr{Z}u^2+2\lambda\psi\kappa\zeta uv-2\varepsilon\lambda\psi\kappa\eta uw+\frac{1}{\mathscr{Z}}uw$$
$$=-\left\{\varepsilon\frac{\partial}{\partial x}(\psi p_{xx})+\varepsilon\mu\frac{\partial}{\partial y}(p_{xy})+\mu\frac{\partial}{\partial z}(p_{xz})-\varepsilon^2\lambda\psi^2\Lambda\mathscr{Z}p_{xx}\right.$$
$$\left.+2\varepsilon\lambda\mu\psi\kappa(\zeta p_{xy}-\eta p_{xz})+\frac{\mu}{\mathscr{Z}}p_{xz}\right\}+g_x, \tag{4.5}$$

$$\frac{\partial v}{\partial t}+\frac{\partial}{\partial x}(\psi uv)+\frac{\partial}{\partial y}(v^2)+\frac{\partial}{\partial z}(vw)-\lambda\psi\kappa\zeta(u^2-v^2)-\varepsilon\lambda\psi^2\Lambda\mathscr{Z}uv-\left(\varepsilon\lambda\psi\kappa\eta-\frac{2}{\mathscr{Z}}\right)vw$$
$$=-\left\{\varepsilon\mu\frac{\partial}{\partial x}(\psi p_{xy})+\varepsilon\frac{\partial}{\partial y}(p_{yy})+\mu\frac{\partial}{\partial z}(p_{yz})-\varepsilon\lambda\psi\kappa\zeta P_y^x\right.$$
$$\left.-\varepsilon^2\lambda\mu\psi^2\Lambda\mathscr{Z}p_{xy}-\mu\left(\varepsilon\lambda\psi\kappa\eta-\frac{2}{\mathscr{Z}}\right)p_{yz}\right\}+g_y, \tag{4.6}$$

$$\varepsilon\left\{\frac{\partial w}{\partial t}+\frac{\partial(\psi uw)}{\partial x}+\frac{\partial(vw)}{\partial y}+\frac{\partial w^2}{\partial z}\right\}+\lambda\psi\kappa\eta u^2-\frac{v^2}{\varepsilon\mathscr{Z}}$$
$$-\varepsilon\lambda(\varepsilon\psi^2\Lambda\mathscr{Z}u-\psi\kappa\zeta v)w-\left(\varepsilon^2\lambda\psi\kappa\eta-\frac{\varepsilon}{\mathscr{Z}}\right)w^2$$
$$=-\left\{\varepsilon\mu\frac{\partial}{\partial x}(\psi p_{xz})+\varepsilon\mu\frac{\partial}{\partial y}(p_{yz})+\frac{\partial}{\partial z}(p_{zz})+\varepsilon\lambda\psi\kappa\eta P_z^x\right.$$
$$\left.-\frac{1}{\mathscr{Z}}P_z^y-\varepsilon^2\lambda\mu\psi^2\Lambda\mathscr{Z}p_{xz}+\varepsilon\lambda\mu\psi\kappa\zeta p_{yz}\right\}+g_z, \tag{4.7}$$

where $P_y^x=(p_{xx}-p_{yy})$, $P_z^x=(p_{xx}-p_{zz})$, $P_z^y=(p_{yy}-p_{zz})$.

4.2. *Kinematic conditions*

The basal topography, $F^b=0$, and the free surface of the avalanche, $F^s=0$, are defined by their respective heights above the curvilinear reference, see figure 2,

$$F^b\equiv -z+b(x,y,t)=0, \quad F^s\equiv z-s(x,y,t)=0. \tag{4.8a, b}$$

The kinematic surface equations in dimensional form are

$$\frac{\partial F^b}{\partial t}+\boldsymbol{u}^b\cdot\nabla F^b=0, \quad \frac{\partial F^s}{\partial t}+\boldsymbol{u}^s\cdot\nabla F^s=0. \tag{4.9}$$

It is emphasized that $\boldsymbol{u}^b$ here is the material velocity of particles at the base, but then processes of bed erosion or sedimentation are excluded. In view of this omission, we deduce from (3.12), (4.1), (4.2), (4.4), (4.8) and (4.9) the following non-dimensional curvilinear kinematic conditions for the basal, $z=b(x,y,t)$, and free, $z=s(x,y,t)$, surfaces:

$$\frac{\partial b}{\partial t}+\psi^b u^b\frac{\partial b}{\partial x}+v^b\frac{\partial b}{\partial y}-w^b=0, \quad \frac{\partial s}{\partial t}+\psi^s u^s\frac{\partial s}{\partial x}+v^s\frac{\partial s}{\partial y}-w^s=0. \tag{4.10}$$

4.3. *Traction-free condition at the free surface*

From the definition (3.12) of the gradient of a scalar field and (4.8b), the traction-free condition (2.4a) is $(p^{ij}/\sqrt{g_{(jj)}})(\partial F^s/\partial x^j)\boldsymbol{g}_i=0$. Hence, the traction-free boundary

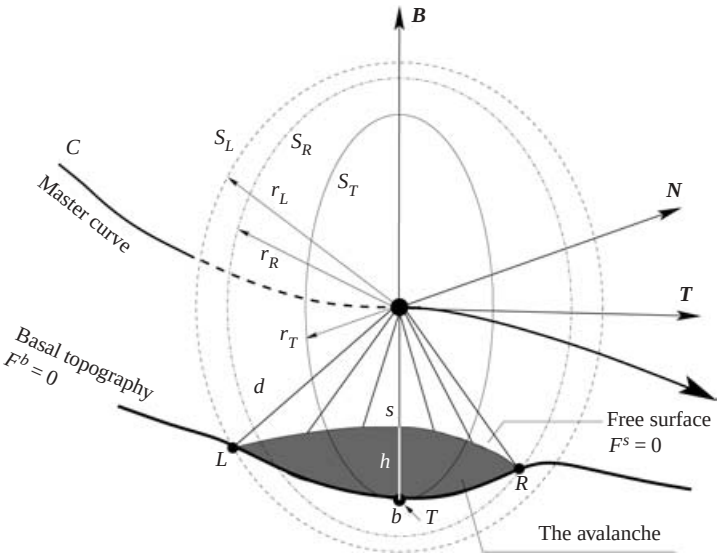

FIGURE 2. For a given value of $s = x$, the avalanche domain in the lateral direction occupies a region in the plane of the circle $S_T \perp C$ distant from the centre of the moving triad $\{\boldsymbol{T}, \boldsymbol{N}, \boldsymbol{B}\}$. The concentric and coplanar circles (with the centre at the master curve and radius r_T, r_R, and r_L), S_T, S_R, and S_L, respectively, pass through the talweg (T) and the left (L) and right (R) marginal points of the avalanche with its basal topography in the lateral direction. The basal topography $F^b = 0$ and the free surface $F^s = 0$ of the avalanche in this plane section are shown. The depth of the avalanche in this section is represented by a height function $h(x, y, t)$ and is measured in the radial direction. Also shown, for instance, is the distance d of the avalanche from the centreline to the circle S_L.

condition at the free surface of the avalanche has downslope, cross-slope and normal (dimensionless) physical components as follows:

$$-\varepsilon\psi^s p^s_{xx}\frac{\partial s}{\partial x} - \varepsilon\mu p^s_{xy}\frac{\partial s}{\partial y} + \mu p^s_{xz} = 0, \tag{4.11a}$$

$$-\varepsilon\mu\psi^s p^s_{yx}\frac{\partial s}{\partial x} - \varepsilon p^s_{yy}\frac{\partial s}{\partial y} + \mu p^s_{yz} = 0, \tag{4.11b}$$

$$-\varepsilon\mu\psi^s p^s_{zx}\frac{\partial s}{\partial x} - \varepsilon\mu p^s_{zy}\frac{\partial s}{\partial y} + p^s_{zz} = 0. \tag{4.11c}$$

4.4. *Coulomb sliding law at the base*

From (3.12), (4.1), (4.2) and (4.4), we obtain the non-dimensional form of the gradient of the basal surface as follows:

$$\nabla F^b = \varepsilon\psi^b\frac{\partial b}{\partial x}\boldsymbol{g}_x + \varepsilon\frac{\partial b}{\partial y}\boldsymbol{g}_y - \boldsymbol{g}_z. \tag{4.12}$$

The Coulomb sliding law (2.4b) implies the relation $\boldsymbol{p}^b\boldsymbol{n}^b = (\boldsymbol{n}^b\cdot\boldsymbol{p}^b\boldsymbol{n}^b)\{(\boldsymbol{u}^b/|\boldsymbol{u}^b|)\tan\delta + \boldsymbol{n}^b\}$. It follows from this and (4.11) and (4.12) that the downslope, cross-slope and normal sliding components, respectively, are

$$\varepsilon\psi^b p^b_{xx}\frac{\partial b}{\partial x} + \varepsilon\mu p^b_{xy}\frac{\partial b}{\partial y} - \mu p^b_{xz} = (\boldsymbol{n}^b\cdot\boldsymbol{p}^b\boldsymbol{n}^b)\left(\Delta_b\frac{u^b}{|\boldsymbol{u}^b|}\tan\delta + \varepsilon\psi^b\frac{\partial b}{\partial x}\right), \tag{4.13a}$$

$$\varepsilon\mu\psi^b p^b_{yx}\frac{\partial b}{\partial x}+\varepsilon p^b_{yy}\frac{\partial b}{\partial y}-\mu p^b_{yz}=(\boldsymbol{n}^b\cdot\boldsymbol{p}^b\boldsymbol{n}^b)\left(\Delta_b\frac{v^b}{|\boldsymbol{u}^b|}\tan\delta+\varepsilon\frac{\partial b}{\partial y}\right), \tag{4.13b}$$

$$\varepsilon\mu\psi^b p^b_{zx}\frac{\partial b}{\partial x}+\varepsilon\mu p^b_{zy}\frac{\partial b}{\partial y}-p^b_{zz}=(\boldsymbol{n}^b\cdot\boldsymbol{p}^b\boldsymbol{n}^b)\left(\Delta_b\frac{\varepsilon w^b}{|\boldsymbol{u}^b|}\tan\delta-1\right), \tag{4.13c}$$

where $|\boldsymbol{u}|=(u^2+v^2+\varepsilon^2w^2)^{1/2}$, the basal unit normal vector $\boldsymbol{n}^b$ is given by $\Delta_b\boldsymbol{n}^b=\nabla F^b$, $\Delta_b:=|\nabla F^b|$, and the associated normalization factor is

$$\Delta_b=\{1+\varepsilon^2(\psi^b)^2(\partial b/\partial x)^2+\varepsilon^2(\partial b/\partial y)^2\}^{1/2}. \tag{4.14}$$

Notice that this dry-friction law could be extended to incorporate a velocity-dependent contribution, but a large number of laboratory experiments have shown an alteration of the sliding law to be unnecessary.

5. Depth integration

The distance between the free surface, $s=s(x,y,t)$, and the basal topography, $b=b(x,y,t)$ defines the thickness, or depth, of the avalanche

$$h(x,y,t)=s(x,y,t)-b(x,y,t), \tag{5.1}$$

measured along the normal direction of the reference surface. A crucial step in deriving the equations of motion for shallow geometry of the granular material is integrating the mass and the momentum-balance equations over the thickness. In order to perform this step, it is useful to define the mean value of a function $f=f(x,y,z,t)$ over the avalanche thickness

$$\bar f(x,y,t)=\frac{1}{h}\int_b^s f(x,y,z,t)\,\mathrm{d}z, \tag{5.2}$$

where the overbar is a shorthand notation for the depth-integrated value divided by the depth. Next, we apply the Leibniz rule to change the order of integration and differentiation, where the square bracket defines the difference of the enclosed function at the two limits of integration, $[f]_a^b=f^b-f^a$.

On using the Leibniz rule the mass balance (4.3) is integrated through the avalanche depth. This yields

$$\begin{aligned}\int_b^s\left\{\frac{\partial}{\partial x}(\psi u)+\frac{\partial v}{\partial y}+\frac{\partial w}{\partial z}-\varepsilon\lambda\psi^2\Lambda\mathscr{Z}u+\lambda\psi\kappa\zeta v-\left(\varepsilon\lambda\psi\kappa\eta-\frac{1}{\mathscr{Z}}\right)w\right\}\mathrm{d}z\\ =\frac{\partial}{\partial x}(h\overline{\psi u})+\frac{\partial}{\partial y}(h\overline{v})-\left[\psi u\frac{\partial z}{\partial x}+v\frac{\partial z}{\partial y}-w\right]_b^s\\ -\varepsilon\lambda h\overline{\psi^2\Lambda\mathscr{Z}u}+\lambda h\overline{\psi\kappa\zeta v}-h\overline{\left(\varepsilon\lambda\psi\kappa\eta-\frac{1}{\mathscr{Z}}\right)w}.\end{aligned}$$

From (4.10) and (5.1) it therefore follows that the depth-integrated form of the mass balance (4.3) takes the form

$$\frac{\partial h}{\partial t}+\frac{\partial}{\partial x}(h\overline{\psi u})+\frac{\partial}{\partial y}(h\overline{v})-\varepsilon\lambda h\overline{\psi^2\Lambda\mathscr{Z}u}+\lambda h\overline{\psi\kappa\zeta v}-h\overline{\left(\varepsilon\lambda\psi\kappa\eta-\frac{1}{\mathscr{Z}}\right)w}=0. \tag{5.3}$$

Depth-integration of the momentum balance equations (4.5)–(4.7) is performed in a number of steps. Integrating the first four terms of the left-hand side of (4.5) (the

downslope acceleration) and using the kinematic conditions (4.10), we have

$$\begin{aligned}
&\int_b^s \left\{ \frac{\partial u}{\partial t} + \frac{\partial}{\partial x}(\psi u^2) + \frac{\partial}{\partial y}(uv) + \frac{\partial}{\partial z}(uw) \right\} \mathrm{d}z \\
&\quad = \frac{\partial}{\partial t}(h\overline{u}) + \frac{\partial}{\partial x}(h\overline{\psi u^2}) + \frac{\partial}{\partial y}(h\overline{uv}) - \left[u \left(\frac{\partial z}{\partial t} + \psi u \frac{\partial z}{\partial x} + v \frac{\partial z}{\partial y} - w \right) \right]_b^s \\
&\quad = \frac{\partial}{\partial t}(h\overline{u}) + \frac{\partial}{\partial x}(h\overline{\psi u^2}) + \frac{\partial}{\partial y}(h\overline{uv}). \qquad (5.4)
\end{aligned}$$

Similarly, the first three terms of the right-hand side of (4.5), after integrating and employing (4.11a) and (4.13a), reduce to

$$\varepsilon \frac{\partial}{\partial x}(h\overline{\psi p_{xx}}) + \varepsilon\mu \frac{\partial}{\partial y}(h\overline{p_{xy}}) + (\boldsymbol{n}^b \cdot \boldsymbol{p}^b \boldsymbol{n}^b) \left(\Delta_b \frac{u^b}{|\boldsymbol{u}^b|} \tan\delta + \varepsilon \psi^b \frac{\partial b}{\partial x} \right), \qquad (5.5)$$

where the Coulomb dry-friction law and the downslope component of the basal normal pressure enter through the boundary conditions. In a similar fashion we can derive corresponding expressions for the depth-integrated cross-slope and normal components of the momentum balances. It then follows that the depth-integrated downslope, cross-slope and normal components of the momentum balances, respectively, are

$$\begin{aligned}
&\frac{\partial}{\partial t}(h\overline{u}) + \frac{\partial}{\partial x}(h\overline{\psi u^2}) + \frac{\partial}{\partial y}(h\overline{uv}) - \varepsilon\lambda h\overline{\psi^2 \Lambda \mathscr{Z} u^2} + 2\lambda\kappa h\overline{\psi \zeta uv} - 2\varepsilon\lambda\kappa h\overline{\psi \eta uw} + h\overline{\left(\frac{uw}{\mathscr{Z}}\right)} \\
&\quad = -\left(\Delta_b \frac{u^b}{|\boldsymbol{u}^b|} \tan\delta + \varepsilon\psi^b \frac{\partial b}{\partial x} \right) (\boldsymbol{n}^b \cdot \boldsymbol{p}^b \boldsymbol{n}^b) - \varepsilon \frac{\partial}{\partial x}(h\overline{\psi p_{xx}}) - \varepsilon\mu \frac{\partial}{\partial y}(h\overline{p_{xy}}) \\
&\qquad + \varepsilon^2\lambda h\overline{\psi^2 \Lambda \mathscr{Z} p_{xx}} - 2\varepsilon\lambda\mu\kappa h\overline{\psi\zeta p_{xy}} + 2\varepsilon\lambda\mu\kappa h\overline{\psi\eta p_{xz}} - \mu h\overline{\left(\frac{p_{xz}}{\mathscr{Z}}\right)} + hg_x, \qquad (5.6) \\
&\frac{\partial}{\partial t}(h\overline{v}) + \frac{\partial}{\partial x}(h\overline{\psi uv}) + \frac{\partial}{\partial y}(h\overline{v^2}) - \lambda\kappa h\overline{\psi\zeta(u^2 - v^2)} - \varepsilon\lambda h(\overline{\psi^2 \Lambda \mathscr{Z} uv} - \kappa\overline{\psi\eta vw}) + 2h\overline{\left(\frac{vw}{\mathscr{Z}}\right)} \\
&\quad = -\left(\Delta_b \frac{v^b}{|\boldsymbol{u}^b|} \tan\delta + \varepsilon \frac{\partial b}{\partial y} \right) (\boldsymbol{n}^b \cdot \boldsymbol{p}^b \boldsymbol{n}^b) - \varepsilon\mu \frac{\partial}{\partial x}(h\overline{\psi p_{xy}}) - \varepsilon \frac{\partial}{\partial y}(h\overline{p_{yy}}) + \varepsilon\lambda\kappa h\overline{\psi\zeta P_y^x} \\
&\qquad + \varepsilon^2\lambda\mu h\overline{\psi^2 \Lambda \mathscr{Z} p_{xy}} + \varepsilon\lambda\mu\kappa h\overline{\psi\eta p_{yz}} + 2\mu h\overline{\left(\frac{p_{yz}}{\mathscr{Z}}\right)} + hg_y, \qquad (5.7) \\
&\varepsilon \left\{ \frac{\partial}{\partial t}(h\overline{w}) + \frac{\partial}{\partial x}(h\overline{\psi uw}) + \frac{\partial}{\partial y}(h\overline{vw}) \right\} + \lambda\kappa h\overline{\psi\eta u^2} - \frac{h}{\varepsilon}\overline{\left(\frac{v^2}{\mathscr{Z}}\right)} - \varepsilon^2\lambda h\overline{\psi^2 \Lambda \mathscr{Z} uw} \\
&\qquad + \varepsilon\lambda\kappa h\overline{\psi\zeta vw} - \varepsilon^2\lambda\kappa h\overline{\psi\eta w^2} + \varepsilon h\overline{\left(\frac{w^2}{\mathscr{Z}}\right)} \\
&\quad = -\left(\Delta_b \frac{\varepsilon w^b}{|\boldsymbol{u}^b|} \tan\delta - 1 \right) (\boldsymbol{n}^b \cdot \boldsymbol{p}^b \boldsymbol{n}^b) - \varepsilon\mu \frac{\partial}{\partial x}(h\overline{\psi p_{xz}}) - \varepsilon\mu \frac{\partial}{\partial y}(h\overline{p_{yz}}) \\
&\qquad - \varepsilon\lambda\kappa h\overline{\psi\left(\eta P_z^x + \mu\zeta p_{yz}\right)} + h\overline{\left(\frac{p_{yy}}{\mathscr{Z}}\right)} + \varepsilon^2\lambda\mu h\overline{\psi^2 \Lambda \mathscr{Z} p_{xz}} - h\overline{\left(\frac{p_{zz}}{\mathscr{Z}}\right)} + hg_z. \qquad (5.8)
\end{aligned}$$

The depth-integrated mass balance (5.3), and the downslope and cross-slope momentum balances (5.6) and (5.7), form the basis of the granular flow equations. The normal component, (5.8), will thereby serve as an auxiliary equation defining the pressure.

6. Ordering

Equations (5.3), (5.6)–(5.8) constitute four scalar field equations for h, u, v and w as unknowns. However, they contain more than just these unknowns because many 'correction terms' arise which are thickness averages of product quantities of h, u, v and w. The number of these unknown variables can be reduced by introducing a further approximation that is based on the ordering of the various terms arising in these equations. Such orders of magnitudes are now assumed for the parameters λ, λ_τ and μ. Realistic avalanche lengths are generally larger than typical radii of curvature and torsion of the topography. Of course, this is not always so, but $0 < \lambda, \lambda_\tau < 1$ is almost everywhere correct. Similarly δ_0 as a typical friction angle is smaller than 45°. So $0 < \mu < 1$ must also hold. Since the aspect ratio is generally much smaller than unity, $\varepsilon \ll 1$, such conditions are fulfilled for

$$\lambda = O(\varepsilon^{\alpha}), \quad \lambda_\tau = O(\varepsilon^{\alpha_\tau}), \quad \mu = O(\varepsilon^{\beta}), \tag{6.1}$$

where $0 < \alpha, \alpha_\tau, \beta < 1$ are realistic for typical topography and coefficients of basal friction. Therefore, the functions ψ and Δ_b from (4.4*a*) and (4.14), respectively, can be estimated by

$$\psi = 1 + O(\varepsilon^{1+\alpha}), \quad \Delta_b = 1 + O(\varepsilon^2). \tag{6.2}$$

The down- and cross-slope components of the depth-averaged momentum balances (5.6) and (5.7) must be approximated to leading and first order in the parameter ε in order to obtain a realizable theory which includes some constitutive properties of granular material. These equations contain a common term that is multiplied by the factor $(\boldsymbol{n}^b \cdot \boldsymbol{p}^b \boldsymbol{n}^b)$. From the z (i.e. normal) component of the momentum balance (5.8), it follows that

$$\left.\begin{aligned} &\boldsymbol{n}^b \cdot \boldsymbol{p}^b \boldsymbol{n}^b = \lambda\kappa h \overline{\psi \eta u^2} + hC - hg_z + O(\varepsilon) = hC - hg_z + O(\varepsilon^{\gamma}), \\ &C = \overline{\left(\frac{p_{zz}}{\mathscr{Z}}\right)} - \overline{\left(\frac{p_{yy}}{\mathscr{Z}}\right)} - \overline{\left(\frac{v^2}{\varepsilon \mathscr{Z}}\right)}, \quad \gamma = \min\{\alpha, \alpha_\tau, \beta\}. \end{aligned}\right\} \tag{6.3}$$

The z-component of the local momentum balance (4.7) also reduces to

$$\frac{\partial}{\partial z}(p_{zz}) = \frac{1}{\mathscr{Z}} p_{yy} - \frac{1}{\mathscr{Z}} p_{zz} + \frac{v^2}{\varepsilon \mathscr{Z}} + g_z + O(\varepsilon^{\gamma}).$$

Integrating this from $z' = z$ to $z' = s$ we obtain (with $\mathscr{Z}' = z' + z_T$)

$$p_{zz} = -\int_z^s \left\{ \frac{1}{\mathscr{Z}'} p_{yy} - \frac{1}{\mathscr{Z}'} p_{zz} + \frac{v^2}{\varepsilon \mathscr{Z}'} + g_z \right\} \mathrm{d}z' + O(\varepsilon^{\gamma}), \tag{6.4}$$

from which it follows that

$$p_{zz}^b = hC - hg_z + O(\varepsilon^{\gamma}). \tag{6.5}$$

In the (SH) theory linear variability of the pressure with depth is assumed. This is fulfilled if $\int_z^s \{p_{yy}/\mathscr{Z}' - p_{zz}/\mathscr{Z}' + v^2/\varepsilon\mathscr{Z}'\}\,\mathrm{d}z' = O(\varepsilon^{\gamma})$, so it follows from (6.4) that

$$p_{zz} = -(s - z)g_z + O(\varepsilon^{\gamma}), \quad p_{zz}^b = -hg_z + O(\varepsilon^{\gamma}). \tag{6.6a, b}$$

Since we are deriving depth-averaged model equations we must somehow eliminate the effects of the normal component w of the velocity field and the normal coordinate z from the balance equations. In typical avalanche flows the dominant deformation takes place mainly in the downhill direction. It is therefore legitimate to assume that p_{xz} and p_{yz} are of order ε and that their variation with z is negligible. With these

assumptions, we have the following results:

$$\overline{(p_{xz}/\mathscr{Z})} = O(\varepsilon), \quad \overline{(p_{yz}/\mathscr{Z})} = O(\varepsilon). \tag{6.7}$$

Due to the depth-averaging and the Boussinesq assumption (see later, § 7), we may also assume that $\overline{(uw/\mathscr{Z})}, \overline{(vw/\mathscr{Z})}, \overline{(w/\mathscr{Z})}$ are negligible. Moreover, since we consider shallow geometry of the basal topography, for shallow curvature and torsion, we may also consider $\lambda\kappa\zeta$ to be negligible.

7. Closure property and velocity profile

The (SH) theory assumes that the downslope and cross-slope pressures vary linearly with normal pressure through the avalanche depth. This is achieved to leading order by the expression

$$p_{xx} = K_x^b p_{zz} + O(\varepsilon^\gamma), \quad p_{yy} = K_y^b p_{zz} + O(\varepsilon^\gamma), \tag{7.1}$$

$$K_x^b = \begin{cases} K_{x_{act}}, & \partial u/\partial x > 0, \\ K_{x_{pass}}, & \partial u/\partial x < 0, \end{cases} \quad K_y^b = \begin{cases} K_{y_{act}}^{x_{act}}, & \partial u/\partial x > 0, \quad \partial v/\partial y > 0, \\ K_{y_{act}}^{x_{pass}}, & \partial u/\partial x < 0, \quad \partial v/\partial y > 0, \\ K_{y_{pass}}^{x_{act}}, & \partial u/\partial x > 0, \quad \partial v/\partial y < 0, \\ K_{y_{pass}}^{x_{pass}}, & \partial u/\partial x < 0, \quad \partial v/\partial y < 0. \end{cases} \tag{7.2}$$

K_x and K_y are called the earth pressure coefficients. Elementary geometrical arguments may be used to determine these values as functions of the internal and basal angles of friction, Hutter *et al.* (1993),

$$K_x = 2\sec^2\phi(1 \mp \sqrt{1 - \cos^2\phi\sec^2\delta}) - 1, \quad K_y = \frac{1}{2}(K_x + 1 \mp \sqrt{(K_x - 1)^2 + 4\tan^2\delta}),$$

where K_x and K_y are *active* during dilatational motion (upper sign) and *passive* during compressional motion (lower sign). Substituting for the normal pressure p_{zz} from (6.6*a*) into (7.1) and integrating through the avalanche depth, the depth-integrated pressures in the downslope and cross-slope directions are, respectively, given by

$$h\overline{p_{xx}} = -K_x g_z h^2/2 + O(\varepsilon^\gamma), \quad h\overline{p_{yy}} = -K_y g_z h^2/2 + O(\varepsilon^\gamma). \tag{7.3}$$

It is assumed that the velocity profiles are approximately uniform through the avalanche depth (Boussinesq 1903 assumption), i.e. all sliding and little differential shearing takes place:

$$\overline{u} = u^b + O(\varepsilon^{1+\gamma}), \quad \overline{v} = v^b + O(\varepsilon^{1+\gamma}), \quad \overline{uv} = u^b v^b + O(\varepsilon^{1+\gamma}). \tag{7.4}$$

These assumptions are supported by various measurements (Dent *et al.* 1998; Keller, Ito & Nishimura 1998; McElwaine & Nishimura 2001; Eckart, Gray & Hutter 2003).

8. Model equations in conservative form

With the ordering of § 6 and the closure property and velocity approximation of § 7, the depth-integrated mass and momentum-balance equations (5.3), (5.6) and (5.7), respectively, reduce to order $\varepsilon^{1+\gamma}$ to

$$\frac{\partial h}{\partial t} + \frac{\partial}{\partial x}(hu) + \frac{\partial}{\partial y}(hv) = 0, \tag{8.1}$$

$$\frac{\partial}{\partial t}(hu) + \frac{\partial}{\partial x}(hu^2) + \frac{\partial}{\partial y}(huv) = hs_x - \frac{\partial}{\partial x}\left(\frac{\beta_x h^2}{2}\right), \tag{8.2}$$

$$\frac{\partial}{\partial t}(hv) + \frac{\partial}{\partial x}(huv) + \frac{\partial}{\partial y}(hv^2) = hs_y - \frac{\partial}{\partial y}\left(\frac{\beta_y h^2}{2}\right), \tag{8.3}$$

where the superscript b is dropped. The factors β_x and β_y are defined as

$$\beta_x = -\varepsilon g_z K_x, \quad \beta_y = -\varepsilon g_z K_y, \tag{8.4}$$

respectively. The terms s_x and s_y represent the net driving accelerations in the downslope and cross-slope directions, respectively, and are given by

$$s_x = g_x - \frac{u}{|\boldsymbol{u}|}\tan\delta(-g_z + \lambda\kappa\eta u^2) + \varepsilon g_z \frac{\partial b}{\partial x}, \tag{8.5}$$

$$s_y = g_y - \frac{v}{|\boldsymbol{u}|}\tan\delta(-g_z + \lambda\kappa\eta u^2) + \varepsilon g_z \frac{\partial b}{\partial y}, \tag{8.6}$$

where $|\boldsymbol{u}| = (u^2 + v^2)^{1/2}$ is the velocity field tangential to the reference (basal) topography and $\eta = \cos(\theta + \varphi(x) + \varphi_0)$, $\zeta = \sin(\theta + \varphi(x) + \varphi_0)$ and $\theta = y/(\varepsilon z_T)$. The first term on the right-hand sides of (8.5) and (8.6) is due to the gravitational acceleration. The second term emerges from the dry Coulomb friction and incorporates the curvature and torsion effects of the bed, the third term is the projection of the topographic variations along the normal direction. Also note that in applications and numerical computations, it is convenient to take the sign of g_z to be negative which corresponds to the upward-pointing normal from the talweg. With this convention, these model equations exactly reproduce the previous equations of Gray *et al.* (1999), as a special case.

Given the master curve, C, the basal topography b, the material parameters δ and ϕ, equations (8.1)–(8.3), which are written in non-dimensional form and constitute a two-dimensional conservative system of hyperbolic equations, allow three independent variables h, the avalanche geometry, u and v, depth-averaged bed-parallel velocity components, to be computed as functions of time and space, once appropriate initial and boundary conditions are prescribed.

9. Discussion, concluding remarks and outlook

The equations (8.1)–(8.3) are formally analogous, and identical, to those of previous derivations under much simpler situations. For $\eta = 1$ and $\zeta = 0$, which correspond to a large distance between the master curve and the talweg and a small azimuthal angle in the cross-sectional plane, these equations reduce to those of Gray *et al.* (1999) and Wieland *et al.* (1999). By varying the azimuthal angle and the distance between the talweg and the master curve it is now possible to analyse the motion of an avalanche in channels with different cross-slope curvatures and widths. Another major advantage of these new model equations is that they include the effect of torsion in the avalanche motion, which could not be achieved by previous models. Therefore, the applicability of the present model equations is much broader than in the previous cases. This has been achieved by use of a different underlying coordinate system. Clearly, for different azimuthal angles the radial directions are not parallel; at this point the present model deviates from previous ones. This implies that the earlier equations of the (SH) model with torsion-free master curves are exactly reproduced when these master curves are very distant. Similarly, whilst the downslope velocity component in the entire cross-section is parallel to the local direction of the master curve, the transverse velocity component follows concentric circles centred on the master curve within the cross-sectional planes. The advantage of this formulation of a depth-averaged avalanche model lies in its flexibility of application. The flow down an inclined plane or within a channel with its axis in a vertical plane but which may be curved can be described, as can the flow down mountain valleys with arbitrarily

curved and twisted talwegs. It is this last application which has motivated us to derive this model, because it is ideally suited to realistic situations in connection with the use of Geographical Information and Visualisation Systems (GIVS).

The next goal should be to perform numerical simulations with the purpose of providing general purpose software for practitioners involved in the prediction of avalanche run-out in mountainous regions. The intention should be the use of the Geographical Information Systems (GIS) from which digitized realistic topographies in mountainous regions are available. With these GIS particular avalanche-prone subregions can be selected and the reference master curve and the cross-sectional topography constructed for individual sites. From a preselected release of a finite mass of gravel or snow at a breaking zone the flow from initiation to run-out could then be determined. This step requires numerical integration via avalanche purpose-built software that incorporates a total-variation-diminishing non-oscillating scheme. Its output could, in a final step, be used in visualization software to identify endangered zones. A multitude of applications could then be investigated with the software. Comparison with observational data in the field such as photographs from helicopters, or a digital video camera positioned at a fixed station, may then become possible.

This paper is dedicated to Professor J. T. Jenkins on the occasion of his 60th birthday. Financial support was provided by the Deutsche Forschungsgemeinschaft through SFB 298: *Deformation and failure of metallic and granular continua*. We thank three anonymous referees for their constructive criticisms and valuable suggestions.

Appendix. Components of gravitational acceleration

Consider the unit orthonormal basis vectors along the coordinate lines:

$$\boldsymbol{g}_x = \boldsymbol{T}(x), \quad \boldsymbol{g}_y = -\zeta \boldsymbol{N}(x) + \eta \boldsymbol{B}(x), \quad \boldsymbol{g}_z = \eta \boldsymbol{N}(x) + \zeta \boldsymbol{B}(x). \tag{A 1}$$

The gravitational vector $\boldsymbol{g}$ can be written in the form

$$\boldsymbol{g} = (0, 0, -g) = 0\boldsymbol{i} + 0\boldsymbol{j} - g\boldsymbol{k}. \tag{A 2}$$

We need to express $\boldsymbol{g}$ in terms of $\{\boldsymbol{g}_i\}$ as follows:

$$\boldsymbol{g} = g_x\boldsymbol{g}_x + g_y\boldsymbol{g}_y + g_z\boldsymbol{g}_z = g[\hat{g}_x\boldsymbol{T} + (-\zeta\hat{g}_y + \eta\hat{g}_z)\boldsymbol{N} + (\eta\hat{g}_y + \zeta\hat{g}_z)\boldsymbol{B}], \tag{A 3}$$

where $\{g_x, g_y, g_z\} = g\{\hat{g}_x, \hat{g}_y, \hat{g}_z\}$ are the coordinates of $\boldsymbol{g}$ with respect to the basis $\{\boldsymbol{g}_i\}$, see (4.1). Let (t_i), (n_i) and (b_i) be the components of the tangent, normal and binormal, respectively, of a given space curve with respect to the standard Cartesian basis $\{\boldsymbol{i}, \boldsymbol{j}, \boldsymbol{k}\}$. We can express the right-hand side of (A 3) in terms of this basis as follows:

$$\begin{aligned}\boldsymbol{g} &= g[\hat{g}_x(t_1\boldsymbol{i} + t_2\boldsymbol{j} + t_3\boldsymbol{k}) + (-\zeta\hat{g}_y + \eta\hat{g}_z)(n_1\boldsymbol{i} + n_2\boldsymbol{j} + n_3\boldsymbol{k}) + (\eta\hat{g}_y + \zeta\hat{g}_z)(b_1\boldsymbol{i} + b_2\boldsymbol{j} + b_3\boldsymbol{k})] \\ &= g[\hat{g}_x t_1 + Q_1 n_1 + Q_2 b_1]\boldsymbol{i} + g[\hat{g}_x t_2 + Q_1 n_2 + Q_2 b_2]\,\boldsymbol{j} + g[\hat{g}_x t_3 + Q_1 n_3 + Q_2 b_3]\boldsymbol{k},\end{aligned}$$

where $Q_1 = (-\zeta\hat{g}_y + \eta\hat{g}_z)$ and $Q_2 = (\eta\hat{g}_y + \zeta\hat{g}_z)$. Comparing the like terms of this equation with (A 2) and solving it we obtain

$$\left.\begin{aligned}\hat{g}_x &= (b_1 n_2 - b_2 n_1)/\Delta, \\ \hat{g}_y &= (t_2(n_1\eta + b_1\zeta) - t_1(n_2\eta + b_2\zeta))/\Delta, \\ \hat{g}_z &= (t_1(b_2\eta - n_2\zeta) - t_2(b_1\eta - n_1\zeta))/\Delta, \\ \Delta &= t_1(n_2 b_3 - b_2 n_3) + t_2(b_1 n_3 - n_1 b_3) + t_3(n_1 b_2 - b_1 n_2).\end{aligned}\right\} \tag{A 4}$$

For notational brevity we will replace $(\hat{g}_x, \hat{g}_y, \hat{g}_z)$ simply by (g_x, g_y, g_z), so that g_x, g_y and g_z represent non-dimensional physical components of gravitational acceleration along downslope, cross-slope and normal directions, respectively.

REFERENCES

Boussinesq, J. 1903 *Théorie Analytique de la Chaleur*, Vol. 2. Gathier-Villars, Paris.

Dean, W. R. 1927 Note on the motion of fluid in a curved pipe. *Phil. Mag.* **4**(7), 208.

Dean, W. R. 1928 The stream-line motion of fluid in a curved pipe. *Phil. Mag.* **5**(7), 673.

Dent, J. D., Burrel, K. J., Schmidt, D. S., Louge, M. Y., Adams, E. E. & Jazbutis, T. G. 1998 Density, velocity and friction measurements in a dry-snow avalanche. *Annal. Glaciol.* **26**, 247–252.

Eckart, W., Gray, J. M. N. T. & Hutter, K. 2003 Particle image velocimetry (PIV) for granular avalanches on inclined planes. In *Dynamic Response of Granular and Porous Materials under Large and Catastrophic Deformations* (ed. K. Hutter & N. Kirchner). Lecture Notes in Applied and Computational Mechanics, vol. 11, pp. 195–218. Springer.

Gammack, D. & Hydon, P. E. 2001 Flow in pipes with non-uniform curvature and torsion. *J. Fluid Mech.* **433**, 357–382.

Germano, M. 1982 On the effect of torsion on helical pipe flow. *J. Fluid Mech.* **125**, 1–8.

Germano, M. 1989 The Dean equations extended to a helical pipe flow. *J. Fluid Mech.* **203**, 289–305.

Gray, J. M. N. T. 2001 Granular flow in partially filled slowly rotating drums. *J. Fluid Mech.* **441**, 1–29.

Gray, J. M. N. T., Wieland, M. & Hutter, K. 1999 Gravity-driven free surface flow of granular avalanches over complex basal topography. *Proc. R. Soc. Lond.* A **455**, 1841–1874.

Greve, R. & Hutter, K. 1993 Motion of a granular avalanche in a convex and concave curved chute: experiments and theoretical predictions. *Phil. Trans. R. Soc. Lond.* A **342**, 573–600.

Greve, R., Koch, T. & Hutter, K. 1994 Unconfined flow of granular avalanches along a partly curved surface. I. Theory. *Proc. R. Soc. Lond.* A **445**, 399–413.

Herrmann, H. J. & Luding, S. 1998 Modeling granular media on the computer. *Continuum Mech. Thermodyn.* **10**, 189–231.

Hsü, K. 1975 On sturzstorms – catastrophic debris streams generated by rockfalls. *Geol. Soc. Am. Bull.* **86**, 129–140.

Hutter, K. & Koch, T. 1991 Motion of a granular avalanche in an exponentially curved chute: experiments and theoretical predictions. *Phil. Trans. R. Soc. Lond.* A **334**, 93–138.

Hutter, K. & Rajagopal, K. R. 1994 On flows of granular materials. *Continuum Mech. Thermodyn.* **6**, 81–139.

Hutter, K., Siegel, M., Savage, S. B. & Nohguchi, Y. 1993 Two-dimensional spreading of a granular avalanche down an inclined plane. I. Theory. *Acta Mech.* **100**, 37–68.

Jenkins, J. T. & Richman, M. W. 1985 Grad's 13-moment system for a dense gas of inelastic spheres. *Arch. Rat. Mech. Anal.* **87**, 355–377.

Jenkins, J. T. & Savage, S. B. 1983 A theory for the rapid flow of identical, smooth, nearly elastic particles. *J. Fluid Mech.* **130**, 186–202.

Keller, S., Ito, Y. & Nishimura, K. 1998 Measurements of the vertical velocity distribution in ping pong ball avalanches. *Annal. Glaciol.* **26**, 259–264.

Klingbeil, E. 1966 *Tensorrechung für Engenieure*. Bibliographisches Institut, Mannheim: Hochschultaschenbücher.

Koch, T., Greve, R. & Hutter, K. 1994 Unconfined flow of granular avalanches along a partly curved chute. II. Experiments and numerical computations. *Proc. R. Soc. Lond.* A **445**, 415–435.

Lang, T. E. & Dent, J. D. 1980 Scale modelling of snow avalanche impact on structures. *J. Glaciol.* **26**(94), 189–196.

Lang, T. E. & Dent, J. D. 1982 Review of surface friction, surface resistance and flow of snow. *Rev. Geophys. Space Phys.* **20**(1), 21–37.

McElwaine, J. & Nishimura, K. 2001 Ping-pong ball avalanche experiments. *Annal. Glaciol.* **32**, 241–250.

Mercier, C. 1963 Sur une representation des surfaces toroidales: applications aux equilibres magnetohydrodynamiques. *Fusion Nuclearie* **3**, 89–98.

Pudasaini, S. P., Eckart, W. & Hutter, K. 2003*a* Gravity-driven rapid shear flows of dry granular masses in helically curved and twisted channels. *Math. Models Meth. Appl. Sci.* **13**(7), 1019–1052.

Pudasaini, S. P., Hutter, K. & Eckart, W. 2003*b* Gravity-driven rapid shear flows of dry granular masses in topographies with orthogonal and non-orthogonal metrics. In *Dynamic Response of Granular and Porous Materials under Large and Catastrophic Deformations* (ed. K. Hutter & N. Kirchner). Lecture Notes in Applied and Computational Mechanics, vol. 11, pp. 43–82. Springer.

Pudasaini, S. P. & Mohring, J. 2002 Mathematical model and experimental validation of free surface size segregation for polydisperse granular materials. *Granular Matter* **4**(2), 45–56.

Savage, S. B. 1989 Flow of granular materials. In *Theoretical and Applied Mechanics* (ed. P. Germain, M. Piau & D. Caillerie), pp. 241–266. Elsevier.

Savage, S. B. & Hutter, K. 1989 The motion of a finite mass of granular material down a rough incline. *J. Fluid Mech.* **199**, 177–215.

Savage, S. B. & Hutter, K. 1991 Dynamics of avalanches of granular materials from initiation to runout. Part I: Analysis. *Acta Mech.* **86**, 201–223.

Solove'v, L. S. & Shafranov, V. D. 1970 Plasma confinement in closed magnetic system. *Rev. Plasma Phys.* **5**, (New York: Consultants Bureau).

Tai, Y. -C., Gray, J. M. N. T. & Hutter, K. 2001 Dense Granular Avalanches: Mathematical Description and Experimental Validation. In *Geomorphological Fluid Mechanics* (ed. N. L. Balmforth & A. Provenzale). Lecture Notes in Physics, vol. 582, pp. 339–366. Springer.

Wieland, M., Gray, J. M. N. T. & Hutter, K. 1999 Channelized free-surface flow of cohessionless granular avalanches in a chute with shallow lateral curvature. *J. Fluid Mech.* **392**, 73–100.

Zabielski, L. & Mestel, A. J. 1998*a* Steady flow in a helically symmetric pipe. *J. Fluid Mech.* **370**, 297–320.

Zabielski, L. & Mestel, A. J. 1998*b* Unsteady blood flow in a helically symmetric pipe. *J. Fluid Mech.* **370**, 321–345.